

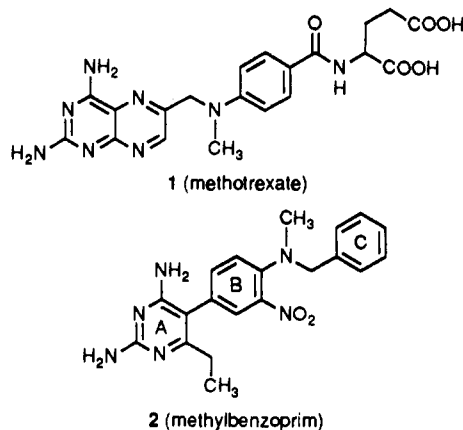
Structural Studies on Bio-active Compounds. 20.^{†‡} Molecular Modeling and Crystallographic Studies on Methylbenzoprim, a Potent Inhibitor of Dihydrofolate Reductase

Brian J. Denny, Neil S. Ringan,[§] Carl H. Schwalbe,* Peter A. Lambert, Michelle A. Meek, Roger J. Griffin,[†] and Malcolm F. G. Stevens

Pharmaceutical Sciences Institute, Department of Pharmaceutical Sciences, Aston University, Aston Triangle, Birmingham B4 7ET, United Kingdom. Received October 10, 1991

Methylbenzoprim (MBP) is a potent inhibitor of dihydrofolate reductase, which is more selective for mammalian than bacterial enzymes. Crystal-structure studies on the free base of MBP, with two independent molecules, and the ethanesulfonate salt, have demonstrated three significantly different conformations for MBP. With the MOPAC optimized MBP cation as starting point, the COSMIC energy was monitored as torsion angles were changed in 5° increments. The barrier to rotation about C(5)-C(11) can create two slowly interconverting rotamers, in agreement with NMR studies. Two conformations of the cation that fit the human DHFR structure from the Brookhaven Protein Data Bank have been found. They differ chiefly by a half-turn about C(5)-C(11), positioning the nitro group on opposite sides but allowing the central and benzylic rings to find hydrophobic surroundings. The central ring is close enough to the predicted position of the cofactor NADPH to make competition likely. Kinetic studies with rat liver DHFR show that MBP is an inhibitor that competes with NADPH as well as dihydrofolate.

Dihydrofolate reductase (DHFR) is an important enzyme in the biosynthesis of DNA. It catalyzes the NADPH-dependent reduction of dihydrofolate to tetrahydrofolate. Since the first use of the antifolate drug methotrexate (MTX) (1) in the 1950s, much attention has been given to new anticancer agents which inhibit the action of the enzyme.^{1,2} Of these a large number contain the 2,4-diaminopyrimidine ring system.³ A promising subset are compounds related to methylbenzoprim⁴ (MBP) (2), which is an inhibitor of dihydrofolate reductase from rat liver comparable in strength to MTX with activity against MTX-resistant murine tumor cell lines.⁵



The three-dimensional structures of DHFR from different species have been determined by X-ray crystallography. These include the enzymes from *E. coli*,^{6,7} *L. casei*,^{6,7} chicken liver,⁸ recombinant human DHFR,^{9,10} and most recently mouse L1210 DHFR.¹¹ These crystal

structures have been used in the design of new agents that can bind to the enzyme.

The aim of this work was to predict the conformation(s) of MBP at the active site of human DHFR, using molecular modeling and quantum mechanical calculations, and to compare this with the known crystal structure of MTX at the active site of DHFR from other species. To validate

- (1) Blaney, J. M.; Hansch, C.; Silipo, C.; Vittorio, A. Structure activity relationships of dihydrofolate reductase inhibitors. *Chem. Rev.* 1984, 84, 333-407.
- (2) Berman, E. M.; Werbel, L. M. The renewed potential for folate antagonists in contemporary cancer chemotherapy. *J. Med. Chem.* 1991, 34, 479-485.
- (3) Blakley, R. L.; Foliates and Pterins In *Chemistry and Biochemistry of Foliates*; Blakley, R. L., Benkovic, S. J., Eds.; Wiley-Interscience: New York, 1985; Vol. 1, Chapter 5.
- (4) Bliss, E. A.; Griffin, R. J.; Stevens, M. F. G. Structural studies on bio-active compounds. Part 5. Synthesis and properties of 2,4-diaminopyrimidine dihydrofolate reductase inhibitors bearing lipophilic azido groups. *J. Chem. Soc., Perkin Trans. 1* 1987, 2217-2228.
- (5) Griffin, R. J.; Meek, M. A.; Schwalbe, C. H.; Stevens, M. F. G. Structural studies on bioactive compounds. 8. Synthesis, crystal structure, and biological properties of a new series of 2,4-diamino-5-aryl-6-ethylpyrimidine dihydrofolate reductase inhibitors with in vivo activity against a methotrexate-resistant tumor cell line. *J. Med. Chem.* 1989, 32, 2468-2474.
- (6) Bolin, J. T.; Filman, D. J.; Matthews, D. A.; Hamlin, R. C.; Kraut, J. Crystal structures of *Escherichia coli* and *Lactobacillus casei* dihydrofolate reductase refined at 1.7-Å resolution. 1. General features and binding of methotrexate. *J. Biol. Chem.* 1982, 257, 13650-13662.
- (7) Filman, D. J.; Bolin, J. T.; Matthews, D. A.; Kraut, J. Crystal structures of *Escherichia coli* and *Lactobacillus casei* dihydrofolate reductase refined at 1.7-Å resolution. 2. Environment of bound NADPH and implications for catalysis. *J. Biol. Chem.* 1982, 257, 13663-13672.
- (8) Matthews, D. A.; Bolin, J. T.; Burrige, J. M.; Filman, D. J.; Volz, K. W.; Kaufman, B. T.; Beddell, C. R.; Champness, J. N.; Stammers, D. K.; Kraut, J. Refined crystal structures of *Escherichia coli* and chicken liver dihydrofolate reductase containing bound trimethoprim. *J. Biol. Chem.* 1985, 260, 381-390.
- (9) Oefner, C.; D'Arcy, A.; Winkler, F. K. Crystal structure of human dihydrofolate reductase complexed with folate. *Eur. J. Biochem.* 1988, 174, 377-385.
- (10) Davies, J. F.; Delcamp, T. J.; Prendergast, N. J.; Ashford, V. A.; Freisheim, J. H.; Kraut, J. Crystal structures of recombinant human dihydrofolate reductase complexed with folate and 5-deazaolate. *Biochemistry* 1990, 29, 9467-9479.
- (11) Groom, C. R.; Thillet, J.; North, A. C. T.; Pictet, R.; Geddes, A. J. Trimethoprim binds in a bacterial mode to the wild type and E30D mutant of mouse dihydrofolate reductase. *J. Biol. Chem.* 1991, 266, 19890-19893.

[†] For part 19 of this series, see: Yates, P. C.; McCall, C. J.; Stevens, M. F. G. Structural Studies on Benzothiazoles. Crystal and Molecular Structure of 5,6-Dimethoxy-2-(4-methoxyphenyl)benzothiazole and Molecular Orbital Calculations on Related Compounds. *Tetrahedron* 1991, 47, 6493-6502.

[‡] Abbreviations: DHFR = dihydrofolate reductase; MBP = methylbenzoprim; *E. coli* = *Escherichia coli*; *L. casei* = *Lactobacillus casei*; MTX = methotrexate; NADPH = β -nicotinamide adenine dinucleotide phosphate, reduced form.

[§] Present address: Department of Molecular and Life Sciences, Dundee Institute of Technology, Bell St., Dundee, DD1 1HG Scotland.

* To whom correspondence should be sent.

[†] Present address: Department of Chemistry, Bedson Building, University of Newcastle upon Tyne, NE1 7RU U.K.

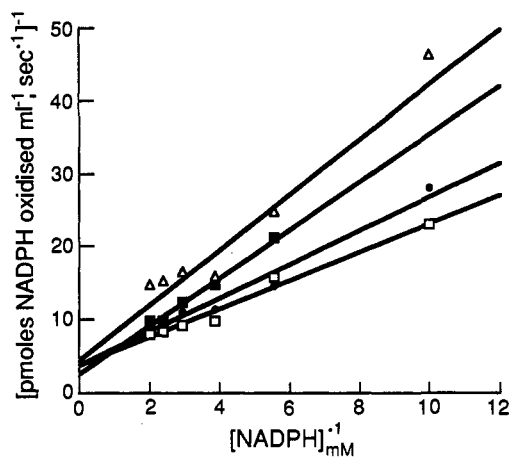


Figure 1. Lineweaver-Burk plot of rate of reaction versus NADPH concentration for different concentrations of MBP. Rate v = pmol of NADPH oxidized $\text{mL}^{-1} \text{s}^{-1}$. \square = no MBP present; \bullet = 25 nM MBP; \blacksquare = 50 nM MBP; \triangle = 100 nM MBP.

the theoretical predictions with experimental data on allowed conformations of MBP, the published crystal structure of its ethanesulfonate salt⁵ has been augmented with a crystal structure determination of the free base of MBP previously available only as an abstract.¹² We also aimed to examine the kinetics of inhibition of rat liver DHFR by MBP.

Biological Activity

Biochemical assays showed that MBP inhibits rat liver DHFR more effectively than *E. coli* DHFR with respective I_{50} values of $9 \times 10^{-9} \text{ M}$ and $900 \times 10^{-9} \text{ M}$. Kinetic studies were performed with the rat liver enzyme. The results are shown in Figure 1 using the method of Lineweaver and Burk¹³ for different concentrations of MBP and NADPH and a fixed saturating level of dihydrofolate ($300 \mu\text{M}$). The results clearly show that MBP and NADPH compete for the same site on the enzyme.

Crystal Structure Determination

The two independent molecules in the crystal structure of MBP base are shown with their numbering scheme as an ORTEP¹⁴ drawing in Figure 2. A hydrogen-bonded dimer is formed in which the 4-amino group of each molecule donates a hydrogen bond to the ring N(3) atom of the other. Translation in the a direction generates another pair of hydrogen bonds between 2-amino groups and N(1) atoms. Such double base-pairing, about a center or a pseudocenter of inversion, is typical of unprotonated diaminopyrimidine antifolates.¹⁵ MBP exhibits very crude pseudocentering, with an angle between pyrimidine ring planes of 32° and an entirely different orientation of the benzylamino substituents on the central benzene ring (B). Torsion angles reveal that the benzyl and nitro substituents emerge from ring B in opposite directions in the unprimed molecule, but gauche in the primed molecule, with additional differences elsewhere along the chain. Another arrangement, with C(13)–C(14)–N(20)–C(22) antiperipla-

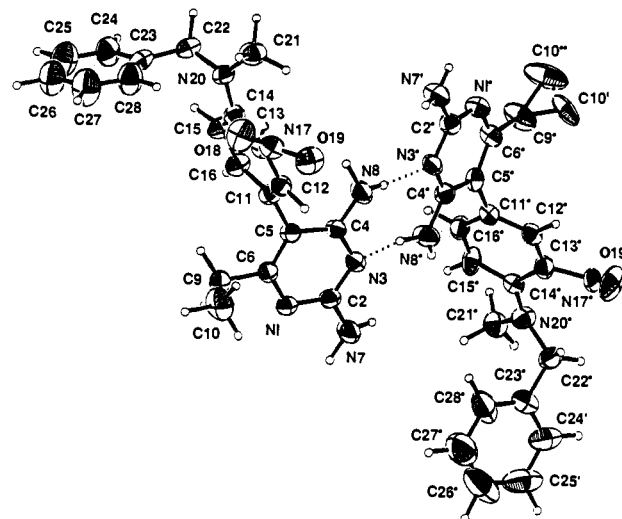


Figure 2. Computer-generated ORTEP drawing of the two independent molecules of methylbenzoprim (2).

nar like the first molecule but otherwise resembling the second, was observed in the ethanesulfonate salt.¹²

Ring B is affected by both the electron-withdrawing nitro group and the electron-donating tertiary amino group. In *N,N*-dimethyl-*m*-nitroaniline,¹⁶ where the substituents do not interact sterically, electronically, or by hydrogen bonding, the C–NO₂ and C–NR₂ distances are 1.492 and 1.404 Å, respectively. In *N,N*-dimethyl-*p*-nitroaniline,¹⁷ which permits electronic interaction, these distances shrink to 1.434 and 1.354 Å averaged over two molecules. In MBP, where electronic interaction also occurs but steric clash and steric inhibition of resonance may stretch these bonds, the values are 1.463 (6) and 1.375 (5) Å for the unprimed molecule, 1.457 (6) and 1.358 (7) Å for the primed. Comparable values are 1.481 (6) and 1.390 (5) Å in the salt.⁵ Thus the nitronate mesomeric form is of moderate importance in MBP, the basicity of the tertiary amino group is somewhat weakened, and it is understandable that the molecule crystallized from ethanesulfonic acid as a singly charged cation protonated only at the N1 position of the diaminopyrimidine ring, not the tertiary arylalkylamine.⁵

Conformational Analysis of MBP

The crystallographic results stimulate further questions: do the various observed orientations of the *N*-benzylamino substituent differ significantly in energy, and is any one of them capable of a good fit to DHFR? The first question was addressed by optimizing the geometry of each conformation by semiempirical molecular orbital techniques (MOPAC¹⁸ with MNDO and PM3 parameters). Only small energy differences (<1.5 kcal mol⁻¹) appeared between the optimized conformations of the two forms of the free base, and also, for comparison, the protonated cation with its proton removed.

Because it is the protonated species that binds to DHFR, the starting point for further work with MBP was taken as the cation from the ethanesulfonate salt, optimized with

(12) Schwalbe, C. H.; Meek, M. A.; Griffin, R. J. Crystal structure and molecular conformation of methylbenzoprim, a novel antifolate drug. *Z. Kristallogr.* 1988, 185, 164.
 (13) Lineweaver, H.; Burk, D. Determination of enzyme dissociation constants. *J. Am. Chem. Soc.* 1934, 56, 658–666.
 (14) Johnson, C. K. ORTEP. Oak Ridge Thermal-Ellipsoid Plot Program. Report ORNL-5136; Oak Ridge National Laboratory: Oak Ridge, TN, 1976.
 (15) Schwalbe, C. H.; Cody, V. Structural studies of antifolate drugs. In *Chemistry and Biology of Pteridines*; Blair, J. A., Ed.; Walter de Gruyter: Berlin, 1983; pp 511–515.

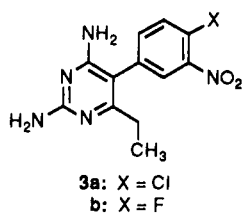
(16) Delugeard, Y.; Messager, J. C. Structure cristalline et moléculaire de la *m*-nitro-*N,N*-diméthylaniline, *Acta Crystallogr.* 1975, B31, 2809–2812.
 (17) Maurin, J.; Krygowski, T. M. Crystallographic studies and physicochemical properties of π -electron systems. Part XIV. Crystal and molecular structure of *N,N*-dimethyl-*p*-nitroaniline. *J. Mol. Struct.* 1988, 172, 413–421.
 (18) Stewart, J. J. P. MOPAC: A semiempirical molecular orbital program. *J. Comput.-Aided Mol. Des.* 1990, 4, 1–105.

MOPAC/MNDO. A fortuitous advantage of this procedure is that the inter-ring torsion angle between rings A and B changed from -105.1° in the crystal structure to -91.2° after optimization. Previously it has been observed that pyrimethamine exhibits an inter-ring torsion angle around 90° , when crystallized within the active site of *E. coli* DHFR.¹⁹

Due to the relatively large number of flexible bonds within MBP, it is conceivable that the conformation which exists at the active site of the enzyme may not correspond to the global minimum, if indeed that is the MOPAC-optimized structure. For example, the heat of formation of the active conformation of MTX taken from the *E. coli* DHFR/MTX crystal structure^{6,7} and optimized with MOPAC keeping torsion angles restrained is 60 kcal mol^{-1} , considerably above the 25 kcal mol^{-1} achieved with full optimization.

To examine the stereochemical relationship of the B and C rings, all the intervening bonds, viz. C(14)–N(20), N(20)–C(22), and C(22)–C(23), along with N(20)–C(21), were systematically rotated pairwise in 20° increments using the COSMIC²⁰ force field within NEMESIS. The results showed that there was considerable flexibility about these bonds. To further define the allowable limits of flexibility, additional conformational analysis was done by changing each torsion angle about C(5)–C(11), C(14)–N(20), N(20)–C(22), and C(22)–C(23) in 5-deg increments keeping the other angles at their MOPAC-optimized levels, and calculating the COSMIC molecular mechanics energy of each conformer. Figure 3 (a–d) shows the calculated energy of MBP as a function of twists about the latter four bonds.

By rotating the C(5)–C(11) bond in MBP it was found, as in earlier studies²¹ on nitropyrimethamine (3a), that the



lowest energy states coincided with C(4)–C(5)–C(11)–C(12) torsion angles of around $+90^\circ$ or -90° , with the highest energy conformations corresponding to torsion angles of 0° or 180° . It is therefore reasonable to assume that two nonequivalent, only slowly interconverting rotamers of MBP can exist, as was observed experimentally during ¹⁹F NMR studies²² on the fluoro analogue of nitropyrimethamine (3b). Extension of this work to other pyrimethamine derivatives and to MBP using ¹H NMR has confirmed this, and has additionally shown that, in the ternary *L. casei* DHFR/MBP/NADP⁺ complex, each of

Table 1^a

	crystal	MOPAC	Enz-1	Enz-2
C(4)–C(5)–C(11)–C(12)	-105.1	-91.2	-89.4	91.8
C(13)–C(14)–N(20)–C(22)	-166.5	-112.7	-127.1	50.0
N(20)–C(22)–C(23)–C(24)	114.4	108.3	85.4	84.9
C(14)–N(20)–C(22)–C(23)	149.0	163.1	65.7	67.2
C(12)–C(13)–N(17)–O(18)	40.4	92.1	99.6	83.7
heat of formation (kcal mol ⁻¹)	276	248	268	279

^a Torsion angles and heats of formation of the MBP crystal structure, the MOPAC-optimized structure, and the two biologically active forms of the molecule. The heats of formation were calculated with version 4 of MOPAC using MNDO parameters.

the two rotamers of MBP can bind to the enzyme and that both bound forms are significantly populated.²³

Torsion angle C(5)–C(6)–C(9)–C(10), which governs the orientation of the ethyl group, attained the value 99.7° in the MNDO-optimized MBP cation, a value found to permit a good fit of 3a to *E. coli* DHFR.²¹ The optimized NO₂ group twisted so as to become nearly perpendicular to ring B. Though likely to be an overestimate, this arrangement minimized the occurrence of artificial, avoidable steric clashes as the C(14)–N(20) bond was rotated with a fixed NO₂ group, and the degree of NO₂ twist had no influence on binding to the enzyme.

Figure 3 shows that the C(14)–N(20) bond can exist in two different states corresponding to torsion angle ranges centered around 60° and -115° . The breadth of these minima is influenced by the steric requirements of the *N*-benzyl and *N*-methyl substituents, while the difference between them of $<180^\circ$ reflects a degree of pyramidalicity of the tertiary amino group.

Docking of Protonated MBP at the Active Site of Human DHFR

The method used was similar to that described previously,²¹ i.e. the MOPAC-optimized MBP cation was positioned in the active site of the human enzyme by superimposing the pyrimidine moieties of the inhibitor and the natural substrate folate. Previous studies have shown that the pteridine ring of methotrexate is inverted relative to folate and dihydrofolate when bound to the *E. coli* enzyme.^{24,25} It has also been shown that 2,4-diaminopyrimidines bind in the same way as methotrexate.^{8,19} Thus the N1 of MBP is positioned where the N3 of folate would normally be and vice versa. Then the folate was removed and the position of the MBP molecule as well as the orientations about its bonds were adjusted while the interaction energy was monitored. Care was taken that the torsion angle changes were all energetically feasible as judged by the energy versus torsion angle graphs of Figure 3.

Two rotameric forms of MBP were found that bound to the enzyme with an interaction energy of -844 and $-781 \text{ kcal mol}^{-1}$. Presumably these correspond to the two different forms that were found in the NMR study with the

- (19) Baker, D. J.; Beddell, C. R.; Champness, J. R.; Goodford, P. J.; Norrington, F. E.; Roth, B.; Stammers, D. K. In *Chemistry and Biology of Pteridines*; Blair, J. A., Ed.; Walter de Gruyter: Berlin, 1983; pp 545–549.
- (20) Vinter, J. G.; Davis, A.; Saunders, M. R. Strategic approaches to drug design. An integrated software framework for molecular modelling. *J. Comput.-Aided Mol. Des.* 1987, 1, 31–51.
- (21) Sansom, C. E.; Schwalbe, C. H.; Lambert, P. A.; Griffin, R. J.; Stevens, M. F. G. Structural studies on bio-active compounds. Part XV. Structure–activity relationships for pyrimethamine and a series of diaminopyrimidine analogues versus bacterial dihydrofolate reductase. *Biochim. Biophys. Acta* 1989, 995, 21–27.
- (22) Tendler, S. J. B.; Griffin, R. J.; Birdsall, B.; Stevens, M. F. G.; Roberts, G. C. K.; Feeney, J. Direct ¹⁹F NMR observation of the conformational selection of optically active rotamers of the antifolate compound fluoronitropyrimethamine bound to the enzyme dihydrofolate reductase. *FEBS Lett.* 1988, 240, 201.

- (23) Birdsall, B.; Tendler, S. B. J.; Arnold, J. R. P.; Feeney, J.; Griffin, R. J.; Carr, M. D.; Thomas, J. A.; Roberts, G. C. K.; Stevens, M. F. G. NMR studies of multiple conformations in complexes of *Lactobacillus casei* dihydrofolate reductase with analogues of pyrimethamine. *Biochemistry* 1990, 29, 9660–9667.
- (24) Fontecilla-Camps, J. C.; Bugg, C. E.; Temple, C.; Rose, J. D.; Montgomery, J. A.; Kisluk, R. L. Absolute configuration of biological tetrahydrofolates. A crystallographic determination. *J. Am. Chem. Soc.* 1979, 101, 6114–6115.
- (25) Charlton, P. A.; Young, D. W.; Birdsall, B.; Feeney, J.; Roberts, G. C. K. Stereochemistry of reduction of folic acid using dihydrofolate reductase. *J. Chem. Soc., Chem. Commun.* 1979, 922–924.

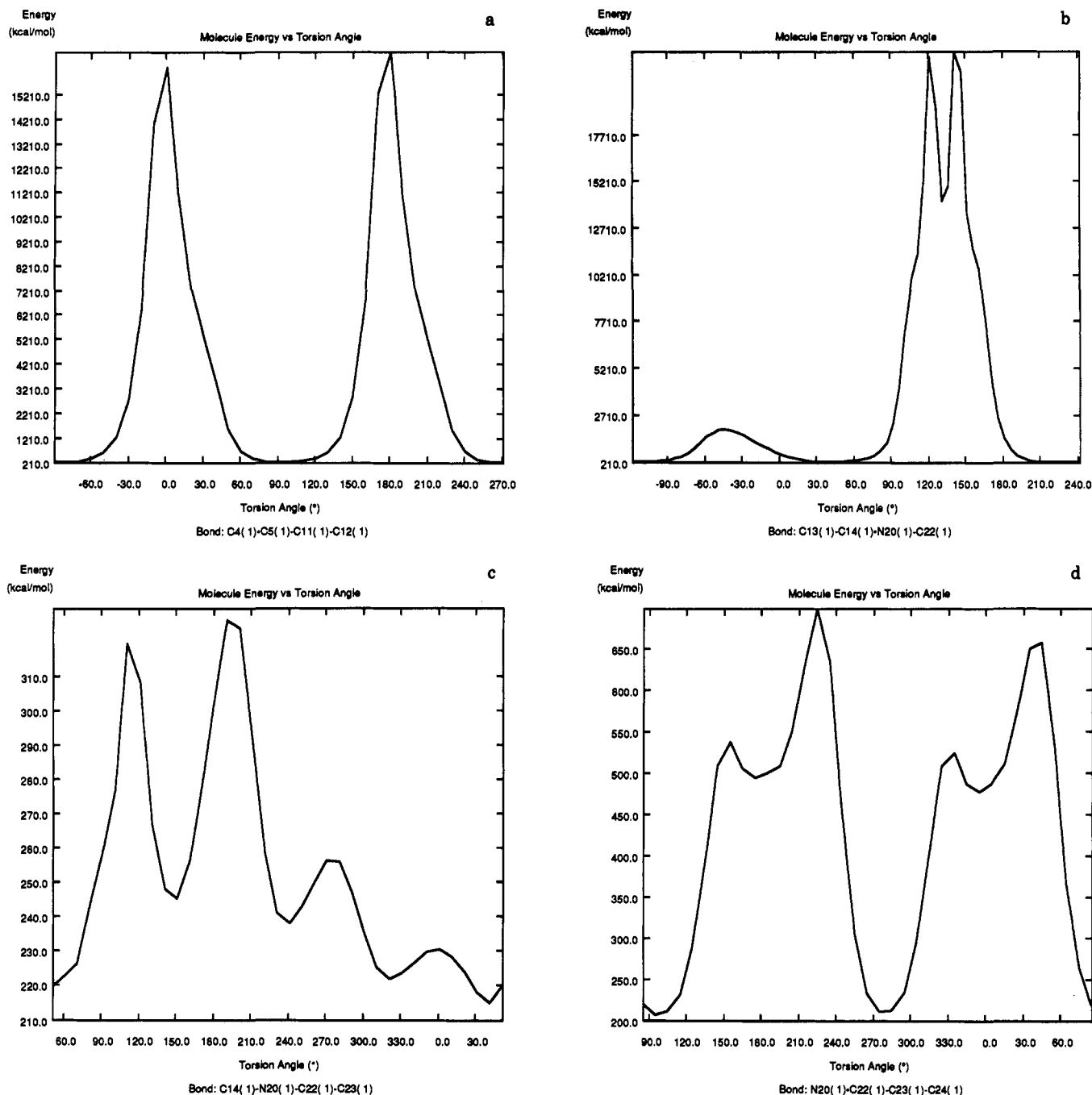


Figure 3. Energy versus torsion angle for the ethanesulfonate salt of MBP optimized with MOPAC (MNDO). Each bond was changed in 5° increments, keeping the other angles fixed. The molecular energy was calculated using the molecular mechanics force field COSMIC. (a) C(4)–C(5)–C(11)–C(12), (b) C(13)–C(14)–N(20)–C(22), (c) C(14)–N(20)–C(22)–C(23), (d) N(20)–C(22)–C(23)–C(24).

L. casei enzyme.²³ These two forms (Enz-1 and Enz-2) only differ significantly in the position of the nitro groups relative to the rest of the molecule. Their respectively antiperiplanar and synclinal disposition of C(13)–C(14)–N(20)–C(22) is reminiscent of the two forms in the crystal structure of the MBP base. Repetition of the conformational analysis in Figure 3 with Enz-1 and Enz-2 as starting points and calculation of the MNDO heat of formation confirmed that the torsion angles for the two conformations correspond to low-energy values and the two forms are energetically feasible. The binding of MTX under the same conditions had an interaction energy of $-641 \text{ kcal mol}^{-1}$ (the structure of MTX being taken from the known crystal structures of enzyme–MTX complexes from *E. coli*^{6,7} without further modification).

The interaction energy that we monitored was based on the electrostatic and van der Waals forces between enzyme

and inhibitor. With no information available in the deposited DHFR structure about the position of solvent molecules, we judged that this simple approach would suffice for the comparison of conformations of the same molecule differing only in the position of relatively hydrophobic groups. However we did include two water molecules that are known to be highly conserved in bacterial (*E. coli*^{6,7} and *L. casei*^{6,7}) as well as chicken liver⁸ and mouse¹¹ enzymes. These waters are known to be important in the binding of other 2,4-diaminopyrimidines.^{8,26}

Table I lists the relevant torsion angles of the two active

(26) Stammers, D. K.; Champness, J. N.; Beddell, C. R.; Dann, J. G.; Eliopoulos, E. E.; Geddes, A. J.; Ogg, D.; North, A. C. T. The structure of mouse L1210 dihydrofolate reductase–drug complexes and the construction of a model of human enzyme. *FEBS Lett.* 1987, 218, 178–184.

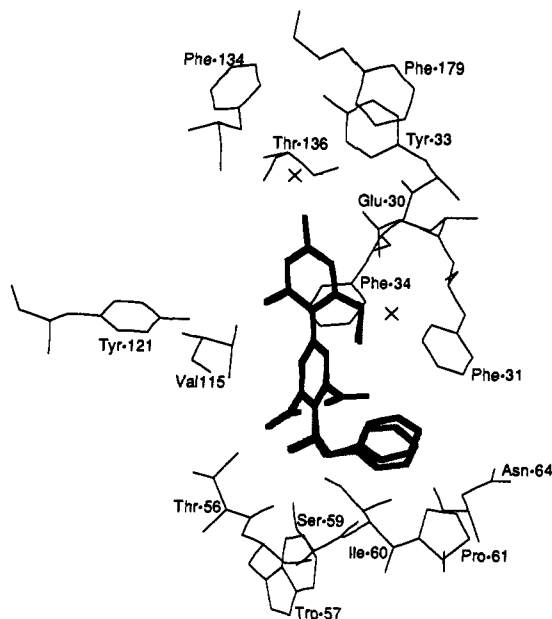


Figure 4. Position of MBP at the active site of human DHFR. The heavy line represents one conformation (Enz-1) and the hashed line represents the other (Enz-2). The x's denote the position of the water molecules.

forms of MBP (Enz-1 and Enz-2) along with the crystal structure and the MOPAC (MNDO) optimized structure of the ethanesulfonate salt.

The proposed active site conformations of the compound (Enz-1 and Enz-2) are shown in Figure 4. In the docked structures, the plane of the central ring B was at a 90° angle to the plane of the pyrimidine ring A, and the plane of the benzyl ring C was at an 80° angle to B.

The proposed binding of the diaminopyrimidine moiety of MBP to human DHFR is in excellent agreement with that reported by Stammers et al. for mouse L1210 DHFR.²⁶ Matthews et al. have shown that there are at least 13 residues involved in the binding of MTX to DHFR from *E. coli*.⁶ In our enzyme-inhibitor model there are 15 residues within 5 Å of the MBP molecule. The most important stabilizing interactions between inhibitor and enzyme are the hydrogen bonding between the diaminopyrimidine moiety and the Glu30, Thr136, Ile7, and Val112 residues of human DHFR (numbering according to the Brookhaven Databank). The two benzene rings both fit into hydrophobic regions, as has also been found for the phenyl ring of pyrimethamine in the *E. coli* active site.²¹ The nearest protein residues are Val115, Phe34, and Trp24 for the ring B and Phe31, Asn64, Pro61, and Leu22 for ring C.

The crystal structure of the enzyme that we used did not contain NADPH. However we did make three predictions of the position of the cofactor based on the homology with the *L. casei*, chicken liver, and mouse enzymes. Each of these structures contained NADPH. The α -carbon chain of each holoenzyme was matched with that of the human enzyme by least squares fit. Removal of the foreign protein left just the human enzyme and NADPH. Notwithstanding some differences in detail, in each case the central ring of MBP occupies the same region of space as the nicotinamide ring of the cofactor. The predicted positions were tested by calculating the interaction energies of folate and MBP in the ternary complex with the human enzyme. The NADPH location based on the mouse structure appeared the most reasonable, giving interaction energies of -197 and +600 kcal mol⁻¹, respectively. These values are consistent with good ternary complex formation

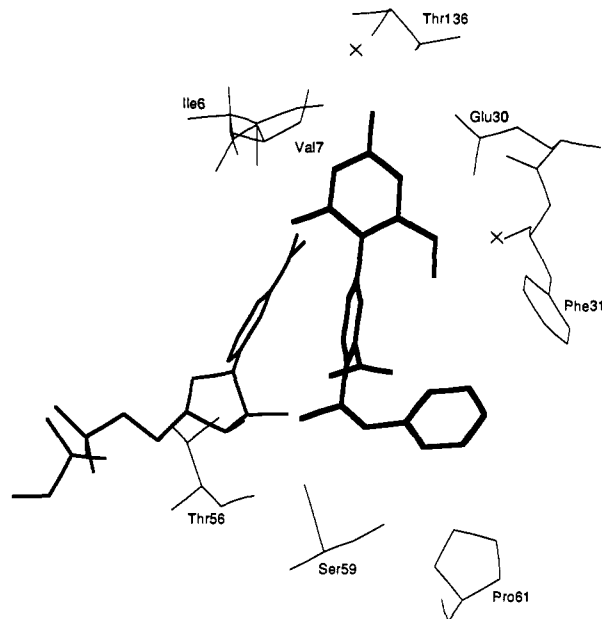


Figure 5. Position of MBP and NADPH at the active site of human DHFR. Position of NADPH based on the position in the mouse enzyme.

by folate but interference between MBP and cofactor. NADPH positions derived from the other two structures are less credible since they gave very large positive interaction energies for both ternary complexes. Figure 5 illustrates the proximity of MPB and NADPH (in the position based on the mouse enzyme). However, until the exact position of NADPH in the human enzyme has been determined crystallographically, we should treat these predictive results with a certain amount of caution.

Kraut's group have shown that a ternary complex is formed between a phenyltriazine inhibitor, NADPH, and chicken liver DHFR.²⁷ They also reported in the same paper that the holoenzyme structure was changed as a result of inhibitor binding. In the present study the predicted position of the cofactor is consistent with our kinetic studies which showed that MBP and NADPH compete for the same site on the enzyme. However, it is not consistent with the NMR results with the bacterial *L. casei* enzyme²³ which showed that both rotameric forms of MBP could form a ternary complex with the enzyme and NADP⁺. While this discrepancy might be attributed to a different orientation of NADP⁺ and NADPH in the binding sites, it may represent a genuine difference in the mode of binding of MPB to mammalian and bacterial DHFR. Subtle differences in enzyme structure can cause remarkable differences in the species selectivity of DHFR inhibitors.²⁸ For example, trimethoprim has a higher affinity for the bacterial enzymes than for vertebrate enzymes,²⁹ whereas for phenyltriazines the trend is reversed.³⁰

Figure 6 shows the comparison between the proposed binding sites for MBP and MTX. The diaminopyrimidine

- (27) Volz, K. W.; Matthews, D. A.; Alden, R. A.; Freer, S. T.; Hansch, C.; Kaufman, B. T.; Kraut, J. Crystal structure of avian dihydrofolate reductase containing phenyltriazine and NADPH. *J. Biol. Chem.* 1982, 257, 2528-2536.
- (28) Burchall, J. J.; Hitchings, G. H. Inhibitor binding analysis of dihydrofolate reductases from different species. *Mol. Pharmacol.* 1965, 1, 126-136.
- (29) Hitchings, G. H.; Burchall, J. J. Inhibition of folate biosynthesis and function as a basis for chemotherapy. *Adv. Enzymol.* 1965, 417-468.
- (30) Baker, B. R. Tissue specific irreversible inhibitors of dihydrofolate reductase. *Acc. Chem. Res.* 1969, 129-136.

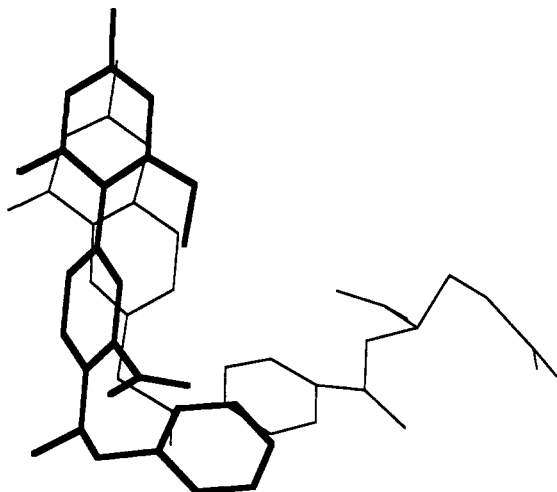


Figure 6. Superimposition of MBP (heavy line) and methotrexate at the active site of human DHFR. For clarity the protein and all the hydrogens have been omitted.

portion of the MBP molecule fits deeper into the protein by about 1 Å. The phenyl and benzyl rings of MBP are roughly perpendicular to the corresponding rings on MTX.

Materials and Methods

MBP crystallized from aqueous 2-ethoxyethanol as hexagonal plates. A specimen $0.80 \times 0.45 \times 0.20$ mm was selected for examination on an Enraf-Nonius CAD4 diffractometer equipped with a graphite monochromator using Mo K α radiation ($\lambda = 0.71069$ Å). Unit cell dimensions were refined by least squares from the setting angles of 25 reflections with $9.7 < \theta < 14.1^\circ$. Crystals exhibit triclinic symmetry, space group $P\bar{1}$, unit cell dimensions $a = 10.563$ (2) Å, $b = 11.842$ (6) Å, $c = 16.158$ (4) Å, $\alpha = 76.35$ (3) $^\circ$, $\beta = 89.53$ (2) $^\circ$, $\gamma = 78.13$ (3) $^\circ$, $V = 1920.3$ Å 3 , $Z = 4$, $D_x = 1.303$ g cm $^{-3}$, $D_m = 1.30$ g cm $^{-3}$ by flotation in CCl $_4$ /light petroleum. Intensity data were collected by ω - 2θ scans for $2 < \theta < 25^\circ$. An empirical absorption correction was applied with the program DIFABS.³¹ The structure was solved by direct methods with MULTAN³² and refined by the full-matrix least-squares technique with SHELX.³³ The terminal C atom of the ethyl substituent on the primed pyrimidine moiety was found to have two alternative positions, C(10') and C(10''). No attempt was made to locate hydrogen atoms in this ethyl group. Although many of the other H atoms did appear in difference electron density maps, methylene and phenyl H atoms were introduced in calculated positions, methyl groups were treated as rotatable rigid bodies, and only the positional parameters of amino H atoms were refined freely. Common isotropic temperature factors were refined for chemically similar H atoms. The two independent molecules were refined alternately in separate blocks with anisotropic thermal parameters for all non-hydrogen atoms. In the weighting scheme $w = k/[\sigma^2(F_o) + gF_o^2]$ the parameters converged to give

$k = 108.53$ and $g = 0$. At termination no shift exceeded 0.06 esd, discrepancy indices were $R = 0.070$, $wR = 0.089$ for 4466 observed reflections ($F > 3\sigma$), and the maximum and minimum features on a difference electron density map were $+0.37$ and -0.30 e Å $^{-3}$. Final non-hydrogen fractional coordinates, bond distances, and bond angles have been deposited as supplementary material.

The coordinates of human DHFR¹⁰ were taken from the Brookhaven Protein Data Bank.³⁴ The geometry of MBP protonated at the N1 position was obtained from the crystal structure of the ethanesulfonate salt and optimized using the COSMIC force field²⁰ with the molecular modeling package NEMESIS³⁶ on an Apple Macintosh IIx machine. These optimized coordinates, along with the crystallographic coordinates of neutral MBP determined in this study, were then transferred to the molecular modeling package CHEM-X³⁶ on a VAX 8650 computer and submitted to the semiempirical molecular orbital package MOPAC with the Modified Neglect of Differential Overlap (MNDO) and PM3 parameters for full and precise geometry optimization and calculation of partial charges.¹⁸ The systematic generation of conformations from the optimized coordinates by rotation of bonds between rings B and C was carried out using the COSMIC force field within the molecular modeling package NEMESIS.

Optimized coordinates and charges were also transferred to NEMESIS for calculation of the energy of rotation about various bonds and to the molecular modeling package QUANTA³⁷ running on an IRIS-3130 workstation (Silicon Graphics) for enzyme docking studies. Conformational analysis was done by changing each torsion angle in 5° increments keeping the other angles at their MOPAC-optimized levels, and calculating the COSMIC molecular mechanics energy of each conformer. As a control of this method we also repeated the experiment using other forms of MBP such as the various crystal structures and the PM3-optimized structure; in each case very similar results were obtained. Partial charges on the protein were calculated using the molecular mechanics package CHARMM.³⁷

The inhibitory activity of MBP against DHFR was determined as described previously²⁸ using cell free enzyme preparations from rat liver²⁸ and *E. coli* MRE 600.³⁸ For all the biological assays, enzyme, inhibitor, and NADPH were preincubated for 5 min at 37 °C before addition of dihydrofolate to allow for formation of the enzyme-inhibitor complex. The I_{50} assays were carried out with saturating levels of NADPH (67 μ M) and dihydrofolate (67 μ M).

Acknowledgment. We thank Mr. Graham Smith for his technical assistance in the preparation of the diagrams and Dr. A. J. Geddes (University of Leeds) for giving us the coordinates of mouse DHFR. This work was supported by the Science and Engineering Research Council under Molecular Recognition Initiative Grant No. GR/F 43635.

Registry No. DHFR, 9002-03-3; MBP, 118344-71-1.

Supplementary Material Available: Tables listing fractional coordinates, bond lengths, and angles for the two independent molecules of MBP in the crystal structure (5 pages). Ordering information is given on any current masthead page.

- (31) Walker, N.; Stuart, D. An empirical method for correcting diffractometer data for absorption effects. *Acta Crystallogr.* 1983, A39, 158.
 (32) Main, P.; Fiske, S. J.; Hull, S. E.; Lessinger, L.; Germain, G.; Declercq, J. P.; Woolfson, M. M. MULTAN 80—A System of Computer Programs for the Automatic Solution of Crystal Structures from X-Ray Diffraction Data. Universities of York and Louvain, 1980.
 (33) Sheldrick, G. M. SHELX 76. Program for Crystal Structure Determination. University of Cambridge, 1976.

- (34) Brookhaven National Laboratory, Upton, NY 11973.
 (35) NEMESIS developed and distributed by Oxford Molecular Ltd., Oxford, U.K.
 (36) CHEMX developed and distributed by Chemical Design Ltd., Oxford, U.K.
 (37) QUANTA and CHARMM developed and distributed by POLY-GEN Corp., Waltham, MA.
 (38) Bertino, J. R.; Fisher, G. A. Techniques for study of resistance to folic acid antagonists. *Methods Med. Res.* 1964, 10, 297-307.